SCIENCE & TECHNOLOGY

A New Genetic Algorithm Based Technique for Biomedical Image Enhancement

Khatkar, Kirti[1*] and Kumar, Dinesh[2]

[1]*Research Scholar, Department of Computer Science & Engineering, GJUS&T, Hissar,Haryana, India*
[2]*Department of Computer Science & Engineering, GJUS&T, Hissar, Haryana, India*

ABSTRACT

From a diagnostic perspective, image enhancement has diverse potential in image processing applications related to biomedical images. A hybrid algorithm obtained by combining discrete wavelet transformation with soft computing techniques is proposed for enhancing the biomedical images. This paper proposes an approach for effective visual enhancement of biomedical images. The proposed approach uses scale-invariant feature transform algorithm and principal component analysis as pre-enhancement steps, followed by the combination of DWT and the genetic algorithm to enhance the biomedical images. In GA, a new fitness function, which can efficiently reduce the noise in biomedical images while preserving the details, is proposed for the enhancement process. In order to accurately evaluate the enhanced image's quality, various metrics like peak signal to noise ratio, contrast to noise ratio, BETA coefficient, standard deviation, and mean square error have been considered. Finally, the comparison of the proposed algorithm with other soft computing techniques like Bacterial Foraging, Particle Swarm Optimization and Fuzzy Logic is carried out. The results show that the proposed technique outperformed over the other methods and provided better image quality.

Keywords: Bacterial foraging, denoizing, standard deviation, Fuzzy logic, genetic algorithm, Haar-wavelet, image enhancement, pre-processing

INTRODUCTION

Various Images like ultrasound, Computed Tomography (CT), and Magnetic Resonance Imaging (MRI) are used globally clinical diagnosis and treatment. Image quality is the key aspect while considering any biomedical image for diagnostic purposes. While capturing the biomedical images, the

noise introduced due to various environmental factors, distorts the captured image quality, in particular damaging the structure and the contents of the image as well as the correlation between pixels. Thus, to remove the noise various pre-processing steps like denoizing, restoration, enhancement, sharpening, and brightness correction are used (Wang, Jiang, & Ning, 2012). For improving the image visualization, enhancement is considered to be of key importance (Takeda, Farsiu, & Milanfar, 2007). However, some enhancement algorithms emphasize only on enhancement than noise reduction, like histogram equalization in wavelet domain (Fu, Lien, & Wong, 2000). Bayesian estimation for multi-component image in wavelet domain (Scheunders & De Backer, 2005), contrast enhancement using modified coarse and detail coefficients (Xiao & Ohya, 2007). Ercelebi and Koc (2006) proposed the lifting-based wavelet domain Wiener filter for noise reduction. Zeng, Dong, Chi and Xu (2004) and Jung et al. (as cited in Claudio & Scharcanski, 2004) proposed wavelet-based methods for both enhancement as well as noise suppression.

The main aim of this paper is to present an effective approach for enhancing the biomedical images for the diagnosis. The blurred biomedical images may lead to wrong diagnosis of diseases, such as lesions in breast cancer diagnosis, tumor detection in brain, and blood vessel thickening. Thus, it becomes imperative to propose a technique that can result in effective image enhancement for a better diagnosis. The advantage of the proposed approach is that it works well on all types of images like ultrasound, MRI, and CT. In the present study, all such images of different human body organs like abdomen, brain, kidney, liver, and lungs have been used. In the pre-enhancement stage, the SIFT and PCA techniques were used. In the second stage a combination of DWT with GA was used for the enhancement purpose. The following section briefly describes wavelets, which are predominantly used for noise reduction.

Wavelet and Biomedical Image Enhancement

Wavelets have been successfully incorporated in various image compression, enhancement, analysis, classification and retrieval applications. Jansene (2001) proposed a wavelet-based denoizing method by using the thresholding concept. Xie, Pierce and Ulaby (2002), and Pizurica, Philips, Lemahieu and Acheroy (2003) proposed the non-homomorphic wavelet filtering techniques for synthetic aperture radar and ultrasound images. Solbo and Eltoft (2004) used homomorphic wavelet filtering of SAR images, which essentially uses logarithmic images instead of the original images, as is the case while dealing with non-homomorphic ones. Later, Selesnick et al. (Selesnick, Baraniuk, & Kingsbury, 2005) proposed a new concept of Dual-Tree Complex Wavelet Transform (DTCWT) for image enhancement. Thavavel and Murugesan (2007) used complex wavelet transform for CT images. Bosdorf, Raupach, Flohr and Hornegger (2008) used the wavelet-based correlation

analysis for CT images to extract the uncorrelated noise component and found that the noise in CT images is non-white.

Tan and Shi (2009) and Anand and Sahambi (2010) used wavelet-based filters for the removal of rician noise that was predominant in MRI images. Later, Wang, Jiang and Xing (2012) proposed a GSM model based wavelet method for CT image denoizing. Xiang-wei, & Yu-xiu, (2015) used wavelet multi-resolution analysis method for image enhancement in which the soft thresholding was applied to obtain an enhanced image. One step further, Rasti, Daneshmand, Alisinanoglu, CagriOzcinar and Anbarjafari (2016) proposed a stationary wavelet transformation for enhancing the image. The previous techniques were used on a single type of image; whereas an effort is being made in the present paper to propose a technique, based on the combination of wavelets and soft computing, which runs well on all kinds of images.

Proposed Work

In this study, we intend to expand the previously suggested methods of enhancements. From the literature review, it is evident that most of the techniques proposed for enhancing the biomedical images are specific to either ultrasound or CT images or MRI images. The technique proposed in this paper works equally well for all kinds of images. By combining the wavelets with soft computing techniques, an effective enhancement technique is proposed for the biomedical images, which would be valuable for diagnostic purposes. This method is divided into two steps: pre-processing step and the main step. Firstly, the SIFT algorithm is implemented on the medical image. The SIFT algorithm is run for as many as hundred iterations on every image under study and the best result in terms of PSNR is considered for PCA application. PCA fully de-correlates the original dataset.

As the energy of a signal mainly lies on the PCA transformed dataset and the random noise is evenly spread over the whole dataset, the signal and noise can be better distinguished in the PCA domain. Thus, PCA is also used as a part of the pre-processing step to enhance SIFT's results.

Pre-processing step

The SIFT and the PCA methods are applied as a pre-processing step in enhancing the medical image.

SIFT (Scale Invariant Feature Transform)

SIFT can vigorously recognize objects among disordered and under incomplete occlusion (Lowe, 2004). Since the SIFT feature descriptor is invariant to uniform scaling and orientation, and partially invariant to illumination changes, it is best suited for feature
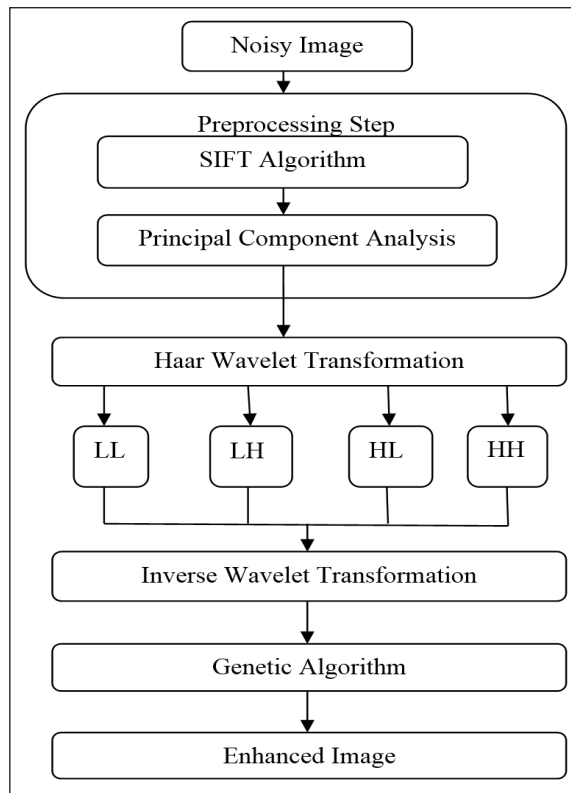
Figure1. Schematic diagram of the proposed method

matching. SIFT key points are first extracted from a set of reference images on the basis of the Euclidean distance of feature vectors. The matching features for the candidate image are extracted.

In the present work when the SIFT algorithm is applied to the noisy biomedical image; the initial image may contain key points that are of low contrast, which is removed by the algorithm. The effect of scale and rotation around each point is removed by selecting areas around every point thus providing better results. For best results, as many as hundred iterations of the SIFT algorithm have been considered individually for different biomedical images. The iteration that gives the highest value for PSNR is considered for further processing. The resultant image is then processed by PCA.

PCA (Principal Component Analysis)

Pearson (1901) proposed PCA as an illustration of the principal axis theorem which was later developed by Harold Hotelling in the 1930 (Hotelling, 1936). The basic logic of PCA is that it converts a set of correlated variables into a set of linearly de-correlated variables called principal components. By using Shannon Entropy (Geiger & Kubin, 2012), PCA reduces the amount of information lost during the dimensionality reduction.

In the proposed work, PCA is applied on the resulting image after SIFT algorithm, it divides the image dataset into principal components that contain the relevant features while the other dataset contains highly uncorrelated noise. PCA low order approximation act as a noise filter by separating correlated features from the uncorrelated noise and preserving them. Thus, it improves the PSNR value in the resulting biomedical image.

Enhancement Method

After performing the pre-processing step on the sample image the Haar wavelet is used for the image enhancement. The wavelet transformation has various properties like good image representation, multi-resolution analysis, data reparability and compaction, which make it a more powerful tool for biomedical image enhancement. In the present approach, the Haar wavelet has been used on the results obtained after applying PCA. The resulting values of various metrics considerably amount of enhance the image. Genetic Algorithm is applied to the Haar results for further optimization of the results.

Enhancement using Wavelets

The use of DWT-based techniques is a recent trend for speckle removal (Bao & Zhang, 2003; Wang, Bovik, Sheikh, & Simoncelli, 2004; Khare, Khare, Yongyeon, Hongkook, & Moongu, 2010). The Haar wavelet is the first known wavelet and was proposed by Alfred Haar in 1909. Its conceptual simplicity, memory efficiency, and reversible nature without edge effect make it more efficient than other wavelets. Due to the multiplicative nature of speckles, the Haar wavelet uses logarithmic transformation to convert multiplicative speckle noise to additive white noise. Subsequently, the wavelet thresholding is used to remove the noise. Later the reverse logarithmic transformation is done (Pizurica et al. 2003). Unlike the traditional method, a combination of wavelets with the GA is used for enhancement purpose in the proposed method. The resulting image after PCA is used as an input for the DWT.

The Haar wavelet is the shortest existing wavelet having a filter for analysis and synthesis of length two due to which the pixel coefficients that lie close to edges, are efficiently retrieved without information loss. As few pixels are used for correlation analysis, noise could be wrongly detected as structures resulting in the appearance of white spots in the Haar wavelet output image. GA is used for further image enhancement. GA has been proven to be a powerful optimization technique in a large solution space and has applications in the biomedical field. The comparison of Haar wavelet with other wavelets for PSNR and MSE is as shown in figures 2(a) and 2(b).The results show that the Haar wavelet provides a better PSNR value than other wavelets, and is hence considered in the proposed method for better results.
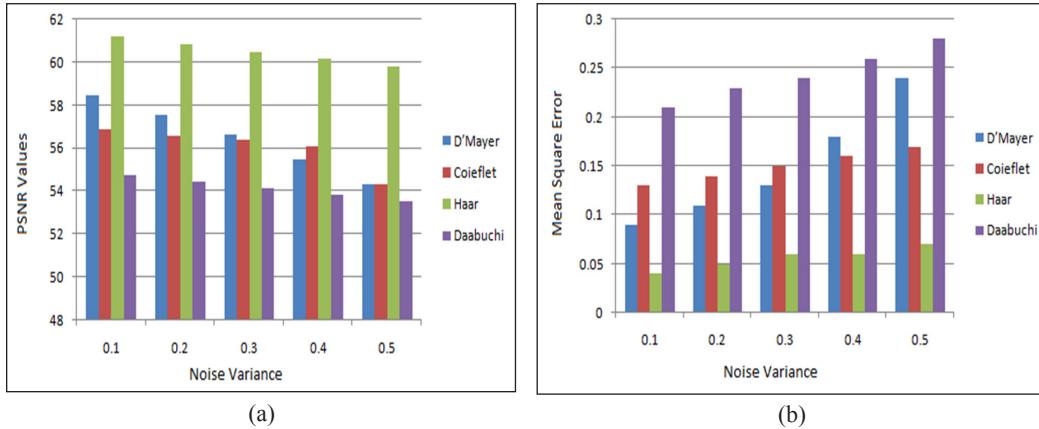
Figure 2. Comparison of different wavelets with the Haar wavelet considering PSNR and MSE

Genetic Algorithms

Genetic algorithms (GA) were developed by John Holland on the basis of the mechanics of natural selection and natural genetics. The GAs are dependent on the concept of "Survival of Fittest". GAs uses a process consisting of selection, crossover and mutation operators. GAs follows the successive generations to choose a chromosome structure. An initial population is randomly generated. Genetic operators, such as crossover and mutation are applied to achieve the desired optimized results (Liu, 2015; Kaur, Gurvinder, & Parminder, 2016).

Steps performed during GA:

1. Initial Population: An initial population of N chromosomes, is randomly generated within the search space. In the initial population, a small number of chromosomes leads to poor results, while a large number results in greater computation time. An optimum number of chromosome population is desirable for good results. Therefore, the number of chromosomes, N, are considered as 50 in the present work and are kept constant in all generations.

2. Fitness Function: In order to evaluate the fitness of chromosomes in every generation the fitness function F_t, which is the average of the summation of each pixel value of the image matrix, is computed by using the formula:

$$F_s = \frac{1}{p}\left[\sum_{j=1}^{p}\frac{1}{q}\left[\sum_{i=1}^{q}a_{i,j}\right]\right]$$

(1)

where p is the number of rows and q is the number of columns in an image matrix.

3. Crossover and Mutation: Genetic crossover is a probabilistic process that exchanges information between two parent chromosomes for generating two child chromosomes.

The arithmetic crossover which produces two complementary linear combinations of the parents selected chromosomes is replaced by new chromosomes that are derived after application of genetic operators. Finally, the results are obtained by choosing the chromosome with the highest fitness value. The results of the proposed method provide better-enhanced images in terms of an increased PSNR value.

Image Quality Assessment

The distortions during acquisition, processing, compression, storage, transmission, and reproduction are responsible for degradation in biomedical images quality. According to Wang, Jiang and Xing (2012) the subjective method of image quality evaluation is inconvenient, time-consuming, and expensive. Therefore, the objective image quality assessment is mainly used in diagnostic applications using quantitative methods to predict the perceived image quality. The important features of image quality assessment like dynamic monitoring and adjusting of image quality, to optimize algorithms and the parameter settings of image processing systems, make it more appropriate for biomedical image applications (Zhang, Wang, & Duanmu, 2010). The enhanced image quality is measured by comparing: peak signal to noise ratio (PSNR), standard deviation (SD), mean square error (MSE), contrast to noise ratio (CNR) and edge detection (BETA).

PSNR of the enhanced image is compared with other images. PSNR is the ratio between the maximum possible power of a signal and the power of corrupting noise that affects the reliability of its representation. It is calculated using Equation 2. The greater the PSNR value the better the image quality.

$$\text{PSNR} = 10\log_{10}\left(\frac{\text{MAX}_1^2}{\text{MSE}}\right) = 20\log_{10}\left(\frac{\text{MAX}_1}{\sqrt{\text{MSE}}}\right)$$

(2)

The beta metric is used as edge and preservation measure in the filtered image (Beis & Lowe, 1997)

$$\beta = \frac{r(\Delta I - \Delta\bar{I}, \Delta\hat{I} - \overline{\Delta\hat{I},)}}{\sqrt{r(I-\Delta\bar{I}, \Delta I - \Delta\bar{I}).r(\Delta\hat{I} - \overline{\Delta\hat{I}}, \Delta\hat{I} - \overline{\Delta\hat{I}}),}}; \left(I_1, I_2\right) = \sum_{(i,j)\in\text{ROI}} I_1(i,j) \cdot I_2(i,j))$$

(3)

where ΔI and $\Delta\hat{I}$ represent the high pass filtered version of original image $I(i,j)$ and its denoizing version $\hat{I}(i,j)$. $\overline{\Delta I}$ and $\overline{\Delta\hat{I}}$ are the mean intensities of ΔI and $\Delta\hat{I}$ respectively. An increasing β indicates a better image quality.

Thirdly the CNR is defined as

$$CNR = \frac{|\mu_d - \mu_u|}{\sqrt{0.5(\sigma_d^2 + \sigma_u^2)}}$$ (4)

Where μ_u and σ_u are the mean, and the SD is computed in an undesired region of interest (UROI), such as background. CNR measurements are proportional to the medical image quality.

We used the SD (the square root of variance) as an estimate of the signal contrast. An unbiased estimate in a discrete form is given by

$$S.D = \sqrt{\frac{1}{N}\sum_{i=1}^{N}(x_i - \mu_x)^2}$$ (5)

MSE shows the average square error between a clean image and an image with error. The lower the MSE, the higher is the denoizing performance. It is given by:

$$MSE = \sum_{i=0}^{R}\sum_{j=0}^{C}\frac{(ls(i,j) - ld(i,j))^2}{R.C}$$ (6)

where, R and C are the dimensions of the image, ls is the original basic test image and ld is the denoized reconstructed image; i and j are the image size coordinates.

RESULTS

In this study, various biomedical images have been used for evaluating the performance of the proposed method. The artificial noise, Gaussian white noise, is added to the original image with a variance of 0.2. The method is compared with other methods used like Fuzzy logic, Particle Swarm Optimization (PSO), Bacterial Foraging Optimization (BFO) (Cincotti, Loi, & Pappalardo, 2001; Passino, 2002). For BFO, the number of bacteria considered in colony is 20, the number of chemotactic steps are 20, the number of reproduction steps are 20, the number of bacteria reproduction per generation is 5, and the elimination dispersion probability is considered 0.9. The below-mentioned table justifies the choice of the above values for different variables for BFO. By keeping the number of chemotactic steps as 20, the number of reproduction steps as 20, the number of bacteria reproduction per generation as 5 and, elimination dispersion probability as 0.9, and by varying the value of the number of bacteria, the PSNR values are as depicted in Table 1.

The PSNR value is the maximum for the bacterial population of 20 and, is therefore considered. Similarly, by keeping the number of bacteria as 20, the number of reproduction steps as 20, the number of bacteria reproduction per generation 5, and the elimination dispersion probability as 0.9 and by varying the value of the number of chemotactic steps, the PSNR values are as depicted in Table 2.

Table 1
Comparison of PSNR values for different population of bacteria for Liver Ultrasound Image

No. of bacteria	10	20	30	40	50
PSNR	65.78103	65.98231	65.28624	65.45401	65.31325

Table 2
Comparison of PSNR values for different chemotactic step for Liver Ultrasound Image

No. of chemotactic step	10	20	30	40	50
PSNR	65.90456	65.98231	65.02596	65.93501	65.70984

The PSNR value is the maximum for the number of chemotactic steps 20, and is therefore considered. Similarly, for different values of elimination-dispersal probability, the reproduction steps and the number of bacteria per generation are depicted in Tables 3, 4 and 5.

Table 3
Comparison of PSNR values for different elimination-dispersal probability for Liver Ultrasound Image

Elimination-dispersal probability	0.9	0.8	0.7	0.6	0.5
PSNR	65.98231	65.35939	65.6964	65.122076	65.30377

Table 4
Comparison of PSNR values for different reproduction step for Liver Ultrasound Image

No. reproduction step	10	20	30	40	50
PSNR	65.92724	65.98231	65.75573	65.80399	65.91268

Table 5
Comparison of PSNR values for different no. of bacteria per generation for Liver Ultrasound Image

No. of bacteria per generation	5	10	15	20	25
PSNR	65.98231	65.1936	65.23485	65.87001	65.45124

From the above tables, it is evident that the best result for BFO is obtained by considering the number of bacteria in the colony as 20, the number of chemotactic steps as 20, the number of reproduction steps as 20, the number of bacteria reproduction per generation as 5, and the elimination dispersion probability as 0.9. Similarly for PSO, the population is initially considered as 100, the number of iterations is 50, and the inertia is 1.0. The results of previous studies show that the wavelets have proven to be an efficient tool for the biomedical image enhancement (Healy, &Weaver, 1991; Sattar, Floreby, Salomonsson, & Lovstrom, 1997).

In the proposed method the various image modalities like MRI, CT, and ultrasound are used for different body organs. MRI imaging uses radio waves and magnets to form an image from inside the body. MRI imaging does not use radiations and produces a greater value for the soft tissues contrast, and is therefore recommended by doctors for the diagnosis of injuries in the brain and heart. The CT scan images, on the other hand, use X-rays to produce cross-sectional images of organs in case of internal injuries. Especially in emergency rooms, as it takes less time to capture CT images. Ultrasound is a radiation free and cheaper technique when compared to CT and MRI imaging that is mainly used for body organs containing less bony structures. In the present study, images of various body organs like heart, brain, abdomen, ovary, pancreas, liver, hepatic and lungs are taken from the University of California, Irvine (UCI) repository dataset and the Science Direct data.

The proposed method with the combination of GA technique offers a considerably improved enhancement capability as compared to the conventional enhancement methods, such as the fast fourier transformation method, the conventional wavelet-based method, and the conventional exponential-Type wavelet coefficient mapping method. The results of various steps of the proposed method for different biomedical images are in Figure 3.
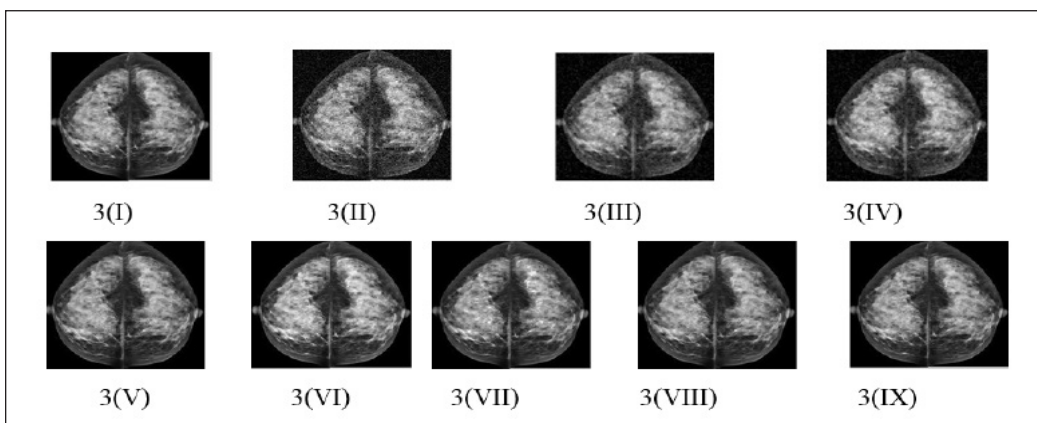

Figure 3 .Results of proposed method (I) original image (II) noisy image (III) SIFT image (IV) PCA image (V) HAAR image (VI) Fuzzy Image (VII) PSO Image (VIII) BFO Image (IX) Resulting image using proposed method for Breast MRI image

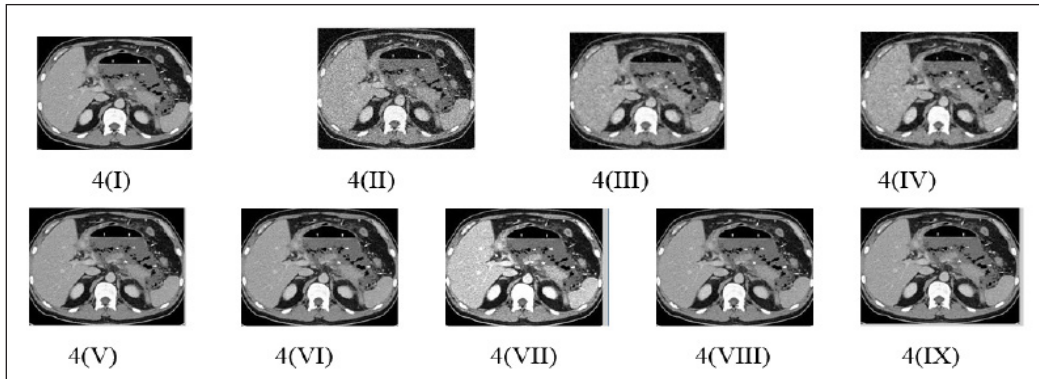The other image considered for study is CT abdomen image shown in Figure 4.

Figure 4. Results of proposed method (I) original image (II) noisy image (III) SIFT image (IV) PCA image (V) HAAR image (VI) Fuzzy Image (VII) PSO Image (VIII) BFO Image (IX) Resulting image using proposed method for CT Abdomen image

Figure 5. Results of proposed method (I) original image (II) noisy image (III) SIFT image (IV) PCA image (V) HAAR image (VI) Fuzzy Image (VII) PSO Image (VIII) BFO Image (IX) Resulting image using proposed method for MRI Brain image

Figure 6. Results of proposed method (I) original image (II) noisy image (III) SIFT image (IV) PCA image (V) HAAR image (VI) Fuzzy Image (VII) PSO Image (VIII) BFO Image (IX) Resulting image using proposed method for MRI Brain   image

Figure 7. Results of proposed method (I) original image (II) noisy image (III) SIFT image (IV) PCA image (V) HAAR image (VI) Fuzzy Image (VII) PSO Image (VIII) BFO Image (IX) Resulting image using proposed method for CT Brain image
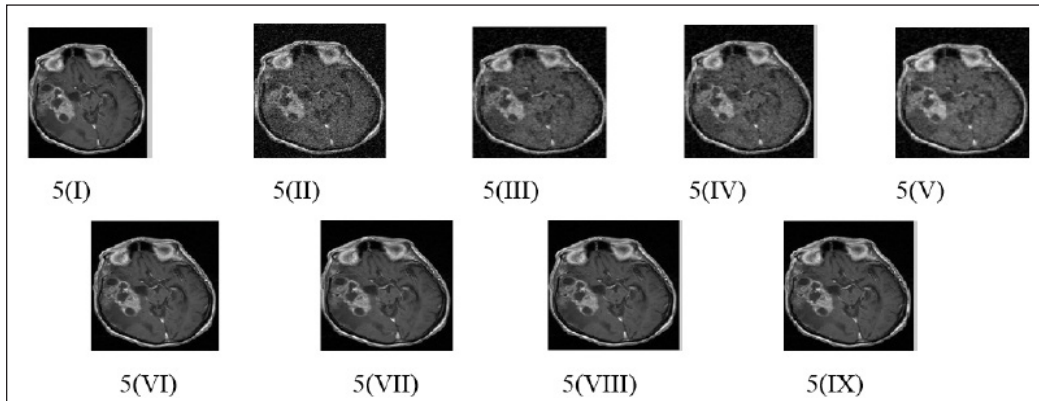

Figure 8. Results of proposed method (I) original image (II) noisy image (III) SIFT image (IV) PCA image (V) HAAR image (VI) Fuzzy Image (VII) PSO Image (VIII) BFO Image (IX) Resulting image using proposed method for CT Lungs image
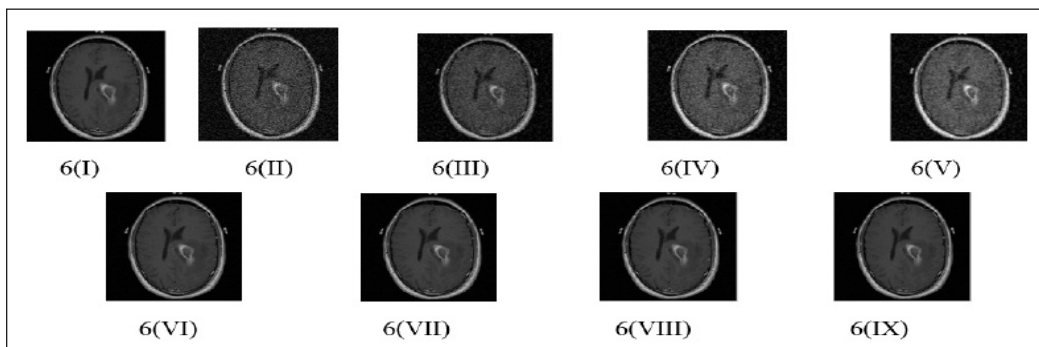

Figure 9. Results of proposed method (I) original image (II) noisy image (III) SIFT image (IV) PCA image (V) HAAR image (VI) Fuzzy Image (VII) PSO Image (VIII) BFO Image (IX) Resulting image using proposed method for CT Rectal image

Figure 10. Results of proposed method (I) original image (II) noisy image (III) SIFT image (IV) PCA image (V) HAAR image (VI) Fuzzy Image (VII) PSO Image (VIII) BFO Image (IX) Resulting image using proposed method for Hepatic MRI image
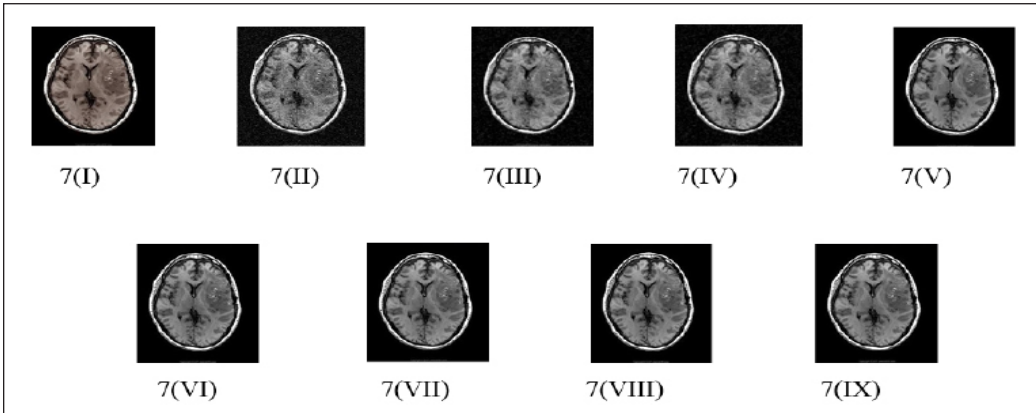

Figure 11. Results of proposed method (I) original image (II) noisy image (III) SIFT image (IV) PCA image (V) HAAR image (VI) Fuzzy Image (VII) PSO Image (VIII) BFO Image (IX) Resulting image using proposed method for Ovary Ultrasound image
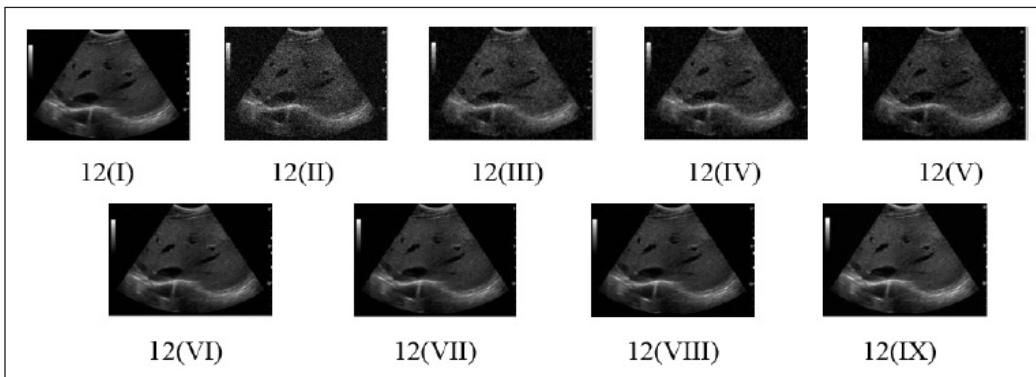
Figure 12. Results of proposed method (I) original image (II) noisy image (III) SIFT image *(IV) PCA* image (V) HAAR image (VI) Fuzzy Image (VII) PSO Image (VIII) BFO Image (IX) Resulting image using proposed method for Pancreas Ultrasound image
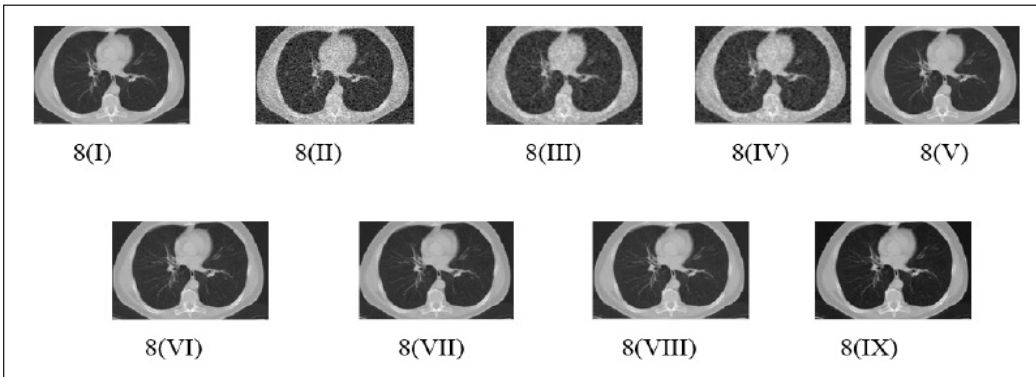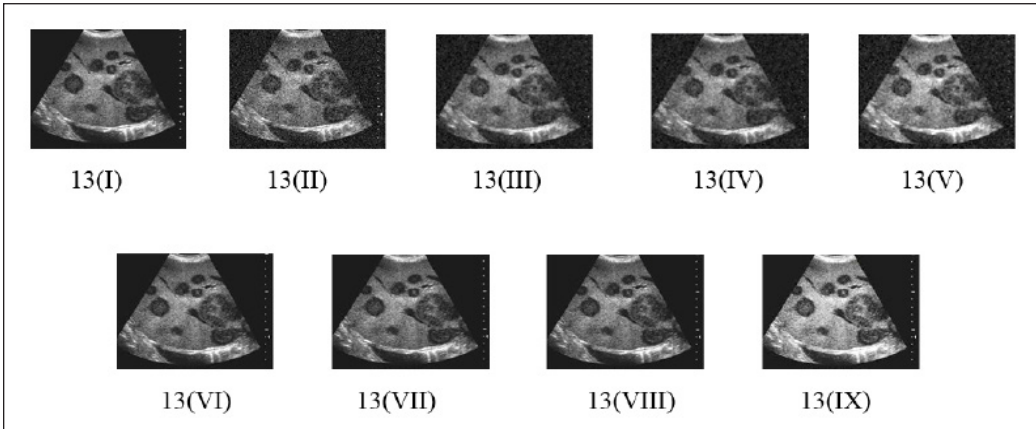
Figure 13. Results of proposed method (I) original image (II) noisy image (III) SIFT image (IV) PCA image (V) HAAR image (VI) Fuzzy Image (VII) PSO Image (VIII) BFO Image (IX) Resulting image using proposed method for Liver Ultrasound image
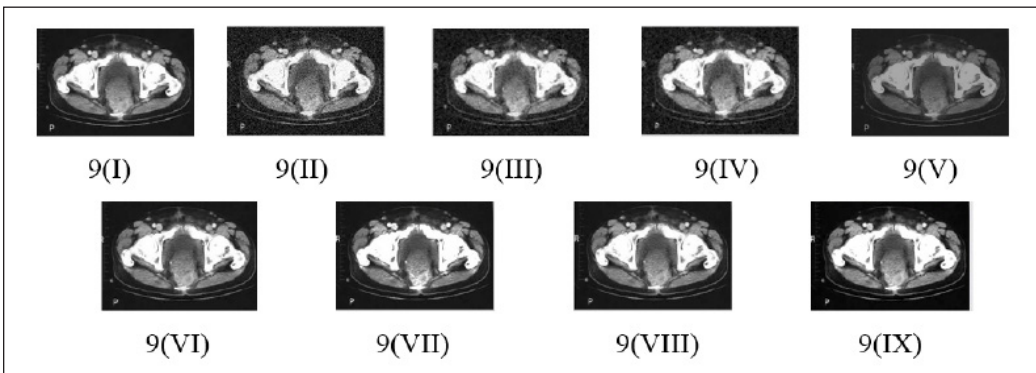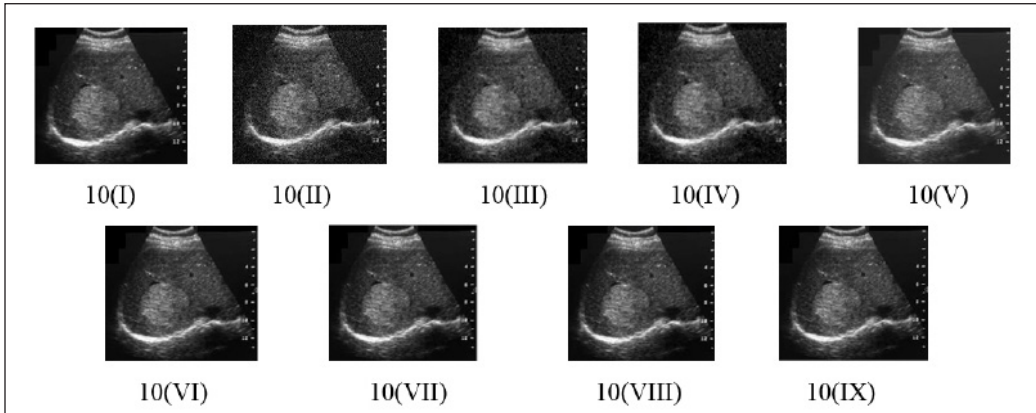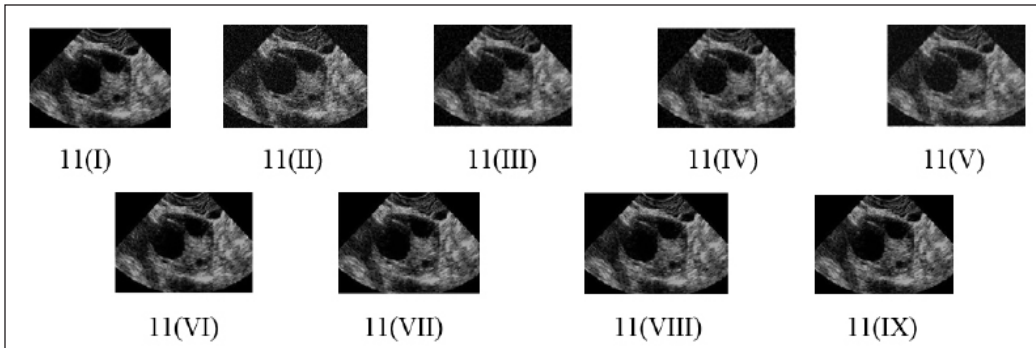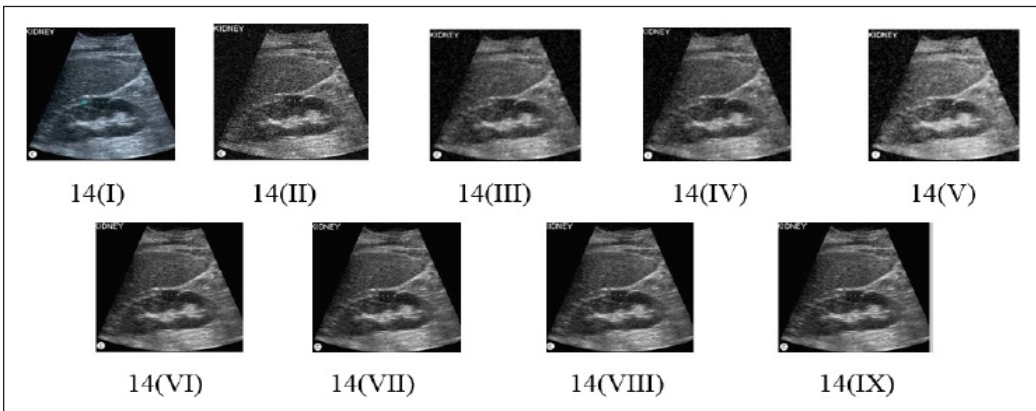

Figure 14. Results of proposed method (I) original image (II) noisy image (III) SIFT image (IV) PCA image (V) HAAR image (VI) Fuzzy Image (VII) PSO Image (VIII) BFO Image (IX) Resulting image using proposed method for Kidney Ultrasound image

In the present study, the hybrid approach is applied on different biomedical images. Figures 3 to 14 illustrate the results of the proposed method and of the Fuzzy, BFO and PSO techniques, at different stages. Tables 6 to 17 represent the comparison of different steps followed in the proposed method and illustrates the significance of each technique used in the pre-processing step, and in the main method. On the basis of the obtained results, it is concluded that the combination of wavelet and GA along with SIFT and PCA can be used as a pre-processing step, and that they can be used as an effective method for biomedical image enhancement. Hence in the proposed method a combination of these techniques has been used for the best results.

Table 6

Comparison of different steps of proposed method for image in figure 3(Breast MRI)

Method	PSNR	MSE	CNR	S.D	BETA
Noisy image + GA	61.6255	0.4472	1.5315	0.7047	2.4532
Noisy image +SIFT +GA	63.1289	0.0316	1.3037	1.9436	1.6792
Noisy image +PCA +GA	60.1186	0.6632	0.8149	1.9324	1.8791
Noisy image +HAAR+ GA	71.5508	0.0045	0.3350	1.0761	2.1716
Noisy image + SIFT +PCA +HAAR+GA	74.1779	0.0024	1.5692	1.7063	1.9132

Table 7

Comparison of different steps of proposed method for image in figure 4(CT Abdomen)

Method	PSNR	MSE	CNR	S.D	BETA
Noisy image + GA	58.2867	0.0964	1.1000	1.2934	1.5307
Noisy image +SIFT +GA	61.1764	0.0495	1.0571	1.9400	1.9722
Noisy image +PCA +GA	58.1661	0.0991	0.0857	1.0135	2.2490
Noisy image +HAAR+ GA	68.1661	0.0099	0.8745	0.7091	2.3735
Noisy image+ SIFT+PCA +HAAR+GA	70.2943	0.0060	0.5575	1.6231	2.1712

Table 8

Comparison of different steps of proposed method for image in figure 5(MRI Brain)

Method	PSNR	MSE	CNR	S.D	BETA
Noisy image + GA	60.4985	0.05647	0.7813	0.1352	1.8142
Noisy image +SIFT +GA	64.1854	0.02574	1.7875	0.2912	2.3179
Noisy image +PCA +GA	63.5120	0.02828	1.6705	0.4782	1.6356
Noisy image +HAAR+ GA	69.8745	0.00931	2.1132	0.1973	1.7452
Noisy image +SIFT+PCA +HAAR+GA	74.5706	0.0022	1.1524	1.6523	1.8867

Table 9

Comparison of different steps of proposed method for image in figure 6(Brain MRI)

Method	PSNR	MSE	CNR	S.D	BETA
Noisy image + GA	62.9897	0.04817	0.8579	0.1255	1.9192
Noisy image +SIFT +GA	65.8142	0.01978	1.8256	0.3197	2.4243
Noisy image +PCA +GA	64.1595	0.02105	1.7254	0.5288	1.7898
Noisy image +HAAR+ GA	70.8232	0.00891	2.2531	0.2173	1.8168
Noisy image+ SIFT+ PCA+ HAAR+GA	74.78	0.0021	1.0000	0.9123	1.2833

Table 10

Comparison of different steps of proposed method for image in figure 7(CT Brain)

Method	PSNR	MSE	CNR	S.D	BETA
Noisy image + GA	61.0483	0.0797	0.83954	1.9869	2.2719
Noisy image +SIFT +GA	64.1727	0.0648	1.3126	0.77882	2.0186
Noisy image +PCA +GA	61.1624	0.0787	1.7638	0.8535	1.6701
Noisy image +HAAR+ GA	68.5885	0.0151	1.6219	1.5406	1.9458
Noisy image+ SIFT+PCA +HAAR+GA	71.0483	0.0051	1.3006	0.9556	1.3436

Table 11

Comparison of different steps of proposed method for image in figure 8(CT Lungs)

Method	PSNR	MSE	CNR	S.D	BETA
Noisy image + GA	58.0538	0.1004	1.6308	2.4277	2.3097
Noisy image +SIFT +GA	61.1210	0.0923	1.754	2.0268	2.471
Noisy image +PCA +GA	58.1107	0.1017	1.8585	0.6978	2.2396
Noisy image +HAAR+ GA	68.0538	0.0101	1.6488	0.6978	2.565
Noisy image+ SIFT+ PCA +HAAR+GA	70.2041	0.0062	0.66034	1.3646	1.4227

Table 12

Comparison of different steps of proposed method for image in figure 9 (CT Rectal)

Method	PSNR	MSE	CNR	S.D	BETA
Noisy image + GA	58.9750	0.0823	0.9612	1.7394	1.9848
Noisy image +SIFT +GA	62.0558	0.0405	1.0254	1.9084	2.0359
Noisy image +PCA +GA	59.0455	0.0810	1.6129	2.0512	2.7698
Noisy image +HAAR+ GA	68.9750	0.00823	1.8612	0.9905	1.5355
Noisy image +SIFT +PCA +HAAR+GA	71.8384	0.0042	1.9019	1.9046	1.9384

Table 13

Comparison of different steps of proposed method for image in figure 10(Hepatic MRI)

Method	PSNR	MSE	CNR	S.D	BETA
Noisy image + GA	61.2160	0.0991	1.5548	2.2252	1.6809
Noisy image +SIFT +GA	64.3450	0.0639	1.0024	0.8737	2.029
Noisy image +PCA +GA	61.3377	0.0878	1.6407	1.7038	2.1821
Noisy image +HAAR+ GA	68.4021	0.0093	1.3917	0.7334	1.9339
Noisy image+ SIFT+PCA +HAAR+GA	71.2160	0.0049	1.1716	0.8736	2.289

Table 14

Comparison of different steps of proposed method for image in figure 11 (Ovary Ultrasound)

Method	PSNR	MSE	CNR	S.D	BETA
Noisy image + GA	58.3367	0.0953	0.4574	1.4241	2.0849
Noisy image +SIFT +GA	62.0152	0.0408	0.8794	0.5477	2.3699
Noisy image +PCA +GA	59.0049	0.08176	1.1855	2.1599	2.0183
Noisy image +HAAR+ GA	68.9391	0.0083	0.7410	0.9701	1.7159
Noisy image+ SIFT+PCA +HAAR+GA	71.7615	0.0043	0.4880	1.4585	2.4271

Table 15

Comparison of different steps of proposed method for image in figure 12(Pancreas Ultrasound)

Method	PSNR	MSE	CNR	S.D	BETA
Noisy image + GA	63.9420	0.0262	1.0638	2.1863	2.1191
Noisy image +SIFT +GA	66.6968	0.0139	0.9293	2.2029	1.2830
Noisy image +PCA +GA	63.6863	0.0278	0.6203	1.6225	2.5112
Noisy image +HAAR+ GA	70.8775	0.0029	0.8984	1.6975	2.4616
Noisy image+ SIFT+PCA+ HAAR+GA	73.4844	0.0010	1.7865	2.3842	2.1429

Table 16

Comparison of different steps of proposed method for image in figure 13 (Liver Ultrasound)

Method	PSNR	MSE	CNR	S.D	BETA
Noisy image + GA	59.8269	0.9676	0.4313	1.8273	2.0343
Noisy image +SIFT +GA	62.9231	0.5033	1.3617	0.8567	2.7824
Noisy image +PCA +GA	59.9128	0.9998	0.0231	0.5617	2.8226
Noisy image +HAAR+ GA	69.8269	0.0067	1.5643	1.4249	2.1231
Noisy image +SIFT +PCA +HAAR+GA	73.6720	0.0027	1.1984	1.9109	2.6094

Table 17

Comparison of different steps of proposed method for image in figure 14 (Kidney Ultrasound)

Method	PSNR	MSE	CNR	S.D	BETA
Noisy image + GA	60.9252	0.8672	1.4699	2.1837	1.6210
Noisy image +SIFT +GA	63.5858	0.4135	0.0896	1.5606	1.7721
Noisy image +PCA +GA	60.5755	0.8998	0.9130	0.4684	2.1451
Noisy image +HAAR+ GA	68.4757	0.0058	0.5896	1.4498	2.5915
Noisy image+ SIFT+PCA+ HAAR+GA	70.4757	0.0019	0.3986	1.0382	2.3327

Tables 6 to 17 represent the numerical results of various evaluation metrics like PSNR, MSE, CNR, S.D and Beta. The above tables justify the combination of different techniques; namely SIFT, PCA, Haar Wavelet and GA in the proposed method. The result of the proposed method has been compared with other soft computing techniques likes, Fuzzy Logic, BFO and PSO. On the basis of the observed values it is concluded that the proposed method provides a better enhancement for biomedical images than other methods. The proposed method provides the best PSNR values for different biomedical images considered under the study. For the first image in table 18, the PSNR value with the proposed method is 74.1779, which is higher than the BFO, Fuzzy and PSO methods, and the method provides the least mean square value of 0.024.The value of CNR, SD and Beta coefficients are also considerably better than Fuzzy Logic and PSO, but slightly less than BFO. In other words the proposed method provides better results than the Fuzzy Logic, PSO, and BFO methods. Tables 18 to 29 also proved that the proposed method provided better results than Fuzzy Logic, PSO and BFO methods.

Table 18

Comparison of different methods for image in figure 3 (Breast MRI)

Method	PSNR	MSE	CNR	S.D	BETA
BFO	65.6237	0.0724	1.9185	1.978	2.3496
PSO	65.7429	0.0368	0.3515	1.716	1.5058
FUZZY LOGIC	66.3927	0.0720	1.5324	0.4556	1.4768
PROPOSED METHOD	74.1779	0.0024	1.6692	1.7063	1.9132

Table 19

Comparison of different methods for image in figure 4 (CT abdomen)

Method	PSNR	MSE	CNR	S.D	BETA
BFO	66.9059	0.1126	1.1521	1.5798	2.7222
PSO	66.6818	0.0932	0.3677	1.1188	2.1685
FUZZY LOGIC	65.8964	0.01753	0.8308	0.4907	2.4058
PROPOSED METHOD	70.2943	0.0060	0.9575	1.3231	2.6712

Table 20

Comparison of different methods for image in figure 5 (Brain MRI)

Method	PSNR	MSE	CNR	S.D	BETA
BFO	66.9999	0.4904	1.7024	0.8362	2.7023
PSO	66.1652	0.0459	0.8373	0.2409	1.6647
FUZZY LOGIC	65.6200	0.0622	0.2080	1.4625	1.5609
PROPOSED METHOD	74.7818	0.0021	1.8477	0.8075	1.9913

Table 21

Comparison of different methods for image in figure 6 (Brain MRI)

Method	PSNR	MSE	CNR	S.D	BETA
BFO	66.8084	0.0588	1.8643	2.3043	2.2736
PSO	66.9261	0.0584	0.6728	1.3759	1.5933
FUZZY LOGIC	66.9046	0.0586	0.1147	2.4150	2.1102
PROPOSED METHOD	74.7780	0.0021	1.8176	1.2337	1.9753

Table 22

Comparison of different methods for image in figure7 (CT Brain)

Method	PSNR	MSE	CNR	S.D	BETA
BFO	65.8392	0.0572	1.3553	0.9526	2.8117
PSO	65.08697	0.0572	0.8639	0.1822	2.0145
FUZZY LOGIC	65.3856	0.0618	0.9267	0.3819	1.4812
PROPOSED METHOD	71.04830	0.0051	1.3006	0.9456	1.3436

Table 23

Comparison of different methods for image in figure 8 (CT Lungs)

Method	PSNR	MSE	CNR	S.D	BETA
BFO	65.2845	0.0923	1.4720	1.2948	2.0162
PSO	65.9062	0.0815	0.4619	0.9737	2.6571
FUZZY LOGIC	66.7110	0.0134	0.9149	0.9964	1.5289
PROPOSED METHOD	70.2041	0.0062	0.9984	1.1646	1.4227

Table 24

Comparison of different methods for image in figure 9 (CT Rectal)

Method	PSNR	MSE	CNR	S.D	BETA
BFO	66.6710	0.1628	1.4452	1.5004	1.4582
PSO	65.0926	0.0763	0.5450	0.6918	2.0368
FUZZY LOGIC	65.4779	0.0468	0.5568	0.7417	1.7675
PROPOSED METHOD	71.8384	0.0042	1.0019	0.9046	1.9384

Table 25

Comparison of different methods for image in figure 10 (Hepatic MRI)

Method	PSNR	MSE	CNR	S.D	BETA
BFO	66.0539	0.0463	0.9778	0.9269	2.7486
PSO	66.3980	0.0051	0.5579	0.0195	2.2353
FUZZY LOGIC	65.2286	0.0113	0.6796	0.3067	1.2499
PROPOSED METHOD	71.2160	0.0049	0.9716	0.8736	2.289

Table 26

Comparison of different methods for image in figure11 (Ovary Ultrasound)

Method	PSNR	MSE	CNR	S.D	BETA
BFO	66.0510	0.0860	1.8832	1.8140	2.6102
PSO	66.0328	0.0931	0.3853	0.1225	2.3759
FUZZY LOGIC	65.4883	0.1034	0.3939	0.7295	2.7056
PROPOSED METHOD	71.7615	0.0043	0.4880	1.4585	2.4271

Table 27

Comparison of different methods for image in figure 12 (Pancreas Ultrasound)

Method	PSNR	MSE	CNR	S.D	BETA
BFO	65.9646	0.2864	1.7865	1.5816	1.9124
PSO	66.4595	0.0327	0.3139	0.8875	2.9031
FUZZY LOGIC	65.5932	0.3689	0.4648	0.9263	2.1423
PROPOSED METHOD	73.4844	0.0010	1.4865	1.3842	2.1429

Table 28

Comparison of different methods for image in figure 13 (Liver Ultrasound)

Method	PSNR	MSE	CNR	S.D	BETA
BFO	65.9823	0.2822	1.4707	1.9006	2.1063
PSO	66.1653	0.0748	0.5245	0.1406	1.8484
FUZZY LOGIC	65.6278	0.3965	0.7342	0.7807	2.4799
PROPOSED METHOD	73.6720	0.0027	1.1984	1.1109	2.6094

Table 29

Comparison of different methods for image in figure 14 (Kidney Ultrasound)

Method	PSNR	MSE	CNR	S.D	BETA
BFO	65.1001	0.2861	1.1367	1.2161	2.6378
PSO	66.0974	0.0653	0.3457	0.5464	2.1403
FUZZY LOGIC	65.0460	0.3186	0.4432	0.6858	2.0307
PROPOSED METHOD	70.4757	0.0019	0.9986	1.0382	2.3327

Figures 3 to 14 show the results obtained by using the proposed method and by using the Fuzzy Logic, PSO and BFO methods. The images processed by the proposed method show the highest ranking. Tables summarize the quantitative evaluation results for the proposed method and other published methods in terms of PSNR, CNR, S.D, MSE and beta metrics. As described in the above section the PSNR, CNR, S.D and beta measurements are proportional to the medical image quality. It is evident from the tables that the images processed by the proposed method give the best results. The pixel curve for the original image and the pixel curve of the image after using the proposed method are shown below for biomedical images. The x-axis represents the number of pixels and the y-axis represents the pixel values of the images. It is evident from Figure 15 that the pixel-value profile of the image processed by the proposed method is more enhanced at the edges than that of the original image. It is also apparent from the figure that the noise has been significantly reduced by employing the proposed method.

DISCUSSION AND CONCLUSION

In this study, we proposed an algorithm which combined the wavelet and GA. The results of the evaluation, as illustrated in Figure 15.

Figures 3 to 14, suggest that the proposed method is significantly superior to the other methods. It is apparent that the proposed method combines the advantages of the two methods: denoizing and contrast enhancement. The results of the quantitative evaluation also reveal that the proposed method outperformed over the other methods. The main advantage of the proposed approach is that it works on all types of images like CT, MRI and Ultrasound images etc. Although the proposed method provides better PSNR and MSE but the value of beta coefficient is not satisfactory. Secondly, the proposed method is a time consuming process and is very complex. Hence, the proposed method can be simplified in such a way that the complexity and execution time can be reduced in future.
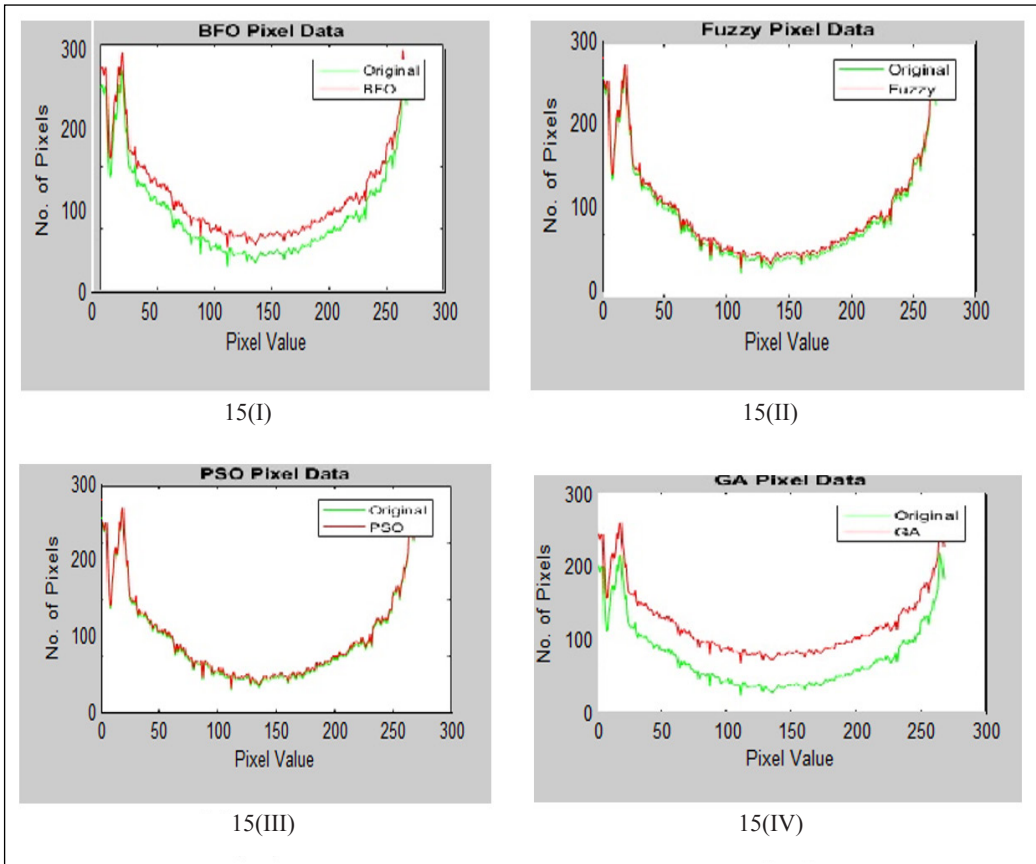
Figure 15. Pixel curve for the biomedical images using original image and Fuzzy Logic, BFO, PSO and with Proposed Method respectively for CT Rectal Image.

REFERENCES

Anand, C. S., & Sahambi, S. (2010). Wavelet domain non-linear filtering for MRI Denoising. *Magnetic Resonance Imaging, 28*(6), 842–861.

Bao, P., & Zhang, L. (2003). Noise reduction for magnetic resonance images via adaptive multiscale products thresholding. *IEEE Transactions on Medical Imaging, 22*(9), 1089–1099.

Beis, J., & Lowe, D. (1997). Shape indexing using approximate nearest -neighbor search in high dimensional spaces. In *Proceedings of the Interational Conference on Computer Vision and Pattern Recognition (CVPR97)* (pp. 1000–1006). Puerto Rico.

Bosdorf, A., Raupach, R., Flohr, T., & Hornegger, J. (2008). Wavelet Based Noise Reduction in CT-Images Using Correlation Analysis. *IEEE Transactions on Medical Imaging, 27*(12), 1685-1703.

Cincotti, G., Loi, G., & Pappalardo, M. (2001). Frequency decomposition and compounding of ultrasound medical images with wavelet packets. *IEEE Transactions on Medical Imaging, 20*(8),764–771.

Claudio, R., & Scharcanski, J. (2004). Wavelet transforms approach to adaptive image denoising and enhancement. *Journal of Electronic Imaging, 13*(2), 278–285.

Ercelebi, E., & Koc, S. (2006). Lifting-based wavelet domain adaptive Wiener filter for image enhancement. *IEEE Proceedings on Vision, Image and Signal Processing, 153*(1), 31–36.

Fu, J. C., Lien, H., & Wong, S. T. C. (2000). Wavelet-based histogram equalization enhancement of gastric sonogram images. *Computerized Medical Imaging and Graphics, 24*(2), 59-68.

Geiger, B., & Kubin, G. (2012). Relative information loss in the PCA. In *Information Theory Workshop (ITW)* (pp. 562-566). Lausanne, Switzerland.

Healy, D. M. Jr., & Weaver, J. B. (1995). Two applications of wavelets and related techniques in medical imaging. *Annals of Biomedical Engineering, 23*(5), 637–65.

Hotelling, H. (1936). Analysis of a complex of statistical variables into principal components. *Journal of Educational Psychology*, 24(6), 417-441.

Jansene, M. (2001). *Noise reduction using wavelets thresholding.. Lecturer series in statistics.* New York: Springer- Verlag.

Kaur, P., Kaur, G., & Parminder (2016). Image enhancement of ultrasound Images using multifarious denoising Filters and GA. In *International Conference on Advances in Computing, Communications and Informatics* (pp. 2375-2384). Jaipur, India.

Khare, A., Khare, M., Yongyeon, J., Hongkook, K., & Moongu, J. (2010). Despeckling of medical ultrasound images using daubechies complex wavelet transform. *Journal of Signal Processing, 90*(2), 428–439.

Lowe, D. (2004). Method and apparatus for identifying scale invariant features in an image and use of same for locating an object in an image. *U.S. Patent No. 6,711,293.* Washington, DC: U.S. Patent and Trademark Office.

Liu, Y. (2015). Image denoising method based on threshold, wavelet transformation and genetic algorithm. *International Journal of Signal Processing, Image Processing and Pattern Recognition, 8*(2), 29-40.

Pearson, K. (1901). On lines and planes of closest fit to systems of points in space. *Philosophical Magazine, 2*(11), 559–572.

Passino, K. M. (2002). Biomimicry of bacterial foraging for distributed optimization and control. *IEEE Control Systems, 22*(3), 52-67.

Pizurica, A., Philips, W., Lemahieu, I., & Acheroy, M. (2003). A versatile wavelet domain noise filtration technique for medical imaging. *IEEE Transactions on Medical Imaging, 22*(3), 323–331.

Rasti, P., Daneshmand, M., Ozcinar, C., & Anbarjafari, G. (2016). Medical image illumination enhancement and sharpening by using stationary wavelet transform. In *24th international conference on Signal Processing and Communication Application Conference (SIU)* (pp. 153-157). Zonguldak, Turkey.

Sattar, F., Floreby, L., Salomonsson, G., & Lovstrom, B. (1997). Image enhancement based on a nonlinear multi- scale method. *IEEE Transactions on Image Processing, 6*(6), 888–895.

Scheunders P., & De Backer, S. (2005). Wavelet-based enhancement of remote sensing and biomedical image series using an auxiliary image. In *Proceedings of SPIE—the international Society for Optical Engineering* (pp. 600105-07). Boston, MA, United States.

Selesnick, W., Baraniuk, R. G., & Kingsbury, N. G. (2005). The Dual-Tree Complex Wavelet Transform. *IEEE Signal Processing Magazine, 22*(6), 123-151.

Solbo, S., & Eltoft, T. (2004). Homomorphic wavelet –based statistical despeckling of SAR images. *IEEE Transactions on Geoscience, Remote Sensing, 42*(4), 711-721.

Takeda, H., Farsiu, S., & Milanfar, P. (2007). Kernel regression for Image Processing and Reconstruction. *IEEE Transactions on Image Processing, 16*(2), 349–366.

Tan, L., & Shi, L. (2009). Multiwavelet-Based Estimation for Improving Magnetic Resonance Images. In *2nd International Congress on Image and Signal Processing* (pp. 1-5). Tianjin, China.

Thavavel, V., & Murugesan, R. (2007). Regularized Computed Tomography using Complex Wavelets. *International Journal of Magnetic Resonance Imaging, 1*(1), 27-32.

Wang, L., Jiang, N., & Xing, N. (2012). Research on medical image enhancement algorithm based on GSM model for Wavelet coefficients. *Physics Procedia, 33*, 1298-1303.

Wang, Z., Bovik, A. C., Sheikh, H. R., & Simoncelli, E. P. (2004). Image quality assessment: from Error visibility to structural similarity. *IEEE Transactions on Image Processing, 13*(4), 600–612.

Xiao, D., & Ohya, J. (2007). Contrast enhancement of color images based on wavelet transform and human visual system. In *Proceedings of the International Conference on Graphics and Visualization in Engineering* (pp. 58–63). Florida, USA.

Xie, H., Pierce, L., & Ulaby, F. T. (2002). Despeckling SAR images using a low –complexity wavelet denoising process**.** In *Geoscience and Remote Sensing Symposium* (pp. 321-324). Toronto, Ontario, Canada.

Xiang-wei, L., & Yu-xiu, K. (2015). A novel medical image enhancement method based on wavelet multi-resolution analysis. In *8th International Conference on Biomedical Engineering and Informatics* (pp. 727-731). Shenyang, China.

Zeng, P. X., Dong, H. Y., Chi, J. N., & Xu, X. H. (2004). An approach for wavelet based image enhancement. In *IEEE International Conference on Robotics and Biometics* (pp. 574–577). Shenyang, China.

Zhang, C., Wang, X., & Duanmu, C. (2010). Adaptive typhoon cloud image enhancement using genetic algorithm and non-linear gain operation in undecimated wavelet domain. *Journal of Engineering Applications of Artificial Intelligence, 23*(1), 61–73.